DesignCon 2010

Additional Trace Losses due to Glass-Weave Periodic Loading

Jason R. Miller
Gustavo J. Blando
Istvan Novak

Sun Microsystems, Inc.
Tel: (781) 442-2274, e-mail: Jason.R.Miller@Sun.com

Abstract

In this paper, we present on a new trace loss mechanism due to the glass-weave. Many PCB laminates are composed of a resin or epoxy material and glass fabric. The electrical properties of these two materials are very different. We examine the impact of the dielectric inhomogeneity on signal loss due to periodic loading of the glass-weave. Periodic loading results in a fundamental resonance where the distance between the discontinuities is one half of a wavelength. Periodic trace loading due to the glass weave and the effects of it have been previously ignored by the literature presumably due to the relatively high half-wave resonance it will establish. A number of key factors, which will be presented in detail, make this effect important to fully characterize and understand now. Due to these factors, glass-weave periodic loading can introduce additional losses in the insertion loss at midrange frequencies. These additional losses will be characterized in the paper using actual glass weave cross-sectional data. Parametric dependencies will be explored. The paper will also show how trace route angle and length can set up different secondary resonance patterns. Among other findings, the paper will show that although forty-five degree routes are preferred to reduce or eliminate glass weave effects, this strategy does not avoid the additional losses due to glass-weave periodic loading and in fact it results in the lowest glass-weave fundamental resonant frequency.

Authors Biography

Jason R. Miller is a senior staff engineer at Sun Microsystems where he works on ASIC development, ASIC packaging, interconnect modeling and characterization, and system simulation. He received his Ph.D. in electrical engineering from Columbia University and has authored or coauthored over 40 technical articles on the topics such as high-speed modeling and simulation. He is co-author of the book "Frequency-Domain Characterization of Power Distribution Networks" published by Artech House in 2007.

Gustavo J. Blando is a staff engineer with over 10 years of experience in the industry. Currently at Sun Microsystems, he is responsible for the development of new processes and methodologies in the areas of broadband measurement, high speed modeling and system simulations. He received his M.S. from Northeastern University.

Istvan Novak is a principle engineer at Sun Microsystems. Besides signal integrity design of high-speed serial and parallel buses, he is engaged in the design and characterization of power-distribution networks and packages for mid-range servers. He creates simulation models, and develops measurement techniques for power distribution. Istvan has twenty plus years of experience with high-speed digital, RF, and analog circuit and system design. He is a Fellow of IEEE for his contributions to signal-integrity and RF measurement and simulation methodologies.

1   Introduction

As data rates continue to increase, there is a greater interest in understanding all elements of the signal path which contribute to the degradation of the signal. In this paper, we present on a new trace loss mechanism due to the glass-weave periodic loading the transmission line.

Many PCB laminates are composed of a resin or epoxy material and glass fabric. The electrical properties of these two materials are very different: glass has very low loss and a dielectric constant near 6. On the other hand, the epoxy has a dielectric loss of about 3% and a dielectric constant around or below 3. A number of publications have examined the impact of this inhomogeneity on differential skew [1, 2], common-mode conversion [2], etc. In this paper, we will examine the impact of the dielectric inhomogeneity on differential and single-ended signal loss due to periodic loading. Periodic loading from the glass weave is due to the periodic nature of the glass weave, which periodically alters both the loss and the dielectric constant along the trace's length.

Periodic loading on transmission lines is a fairly well understood concept [3]. Periodic loading results in a fundamental resonance where the distance between the discontinuities is one half of a wavelength. Harmonics of the fundamental exist at higher frequencies as well. A single repeating loading distance will introduce a peak in the reflection profile and a dip in the insertion loss at the corresponding half-wave resonance frequency. The magnitude of the peak or dip depends on the number of discontinuities and the physical size of the discontinuity. Prior studies have examined the effect of periodic loading, such as plane cutouts or voids, on loss [4] and crosstalk [5].

Periodic trace loading due to the glass weave and the effects of it have been previously ignored by the literature presumably due to the relatively high half-wave resonance it will establish; for a glass weave pitch of 60 mils the half wave resonance in FR4 is about 45 GHz. A number of factors make this effect important to fully characterize and understand now. First, as data rates continue to increase we are getting closer to the fundamental of the glass weave resonance frequency. Second, there can be an additional steepening of the loss profile slope, well below this fundamental resonance, due to the resonance dip. This leads to additional losses in the insertion loss profile due to glass-weave periodic loading at midrange frequencies. Finally, depending on the trace routing path relative to the underlying glass-weave pattern (imagine a trace jogging through a device pin field), resonances can be set up that are well below the fundamental resonance that exists due to the glass weave itself. Also, we will show that even for straight trace routes, lower frequency resonances can be established due to the glass-weave itself, depending on the trace-to-glass-weave angle.

In the paper we will characterize these additional losses using actual glass weave cross-sectional data. Parametric dependencies will be explored using 3D field solvers, including the impact of the glass thickness, proximity to the resin surface, thickness of the glass weave, and pitch of the glass bundles. More than this, we will show how trace route angle and length can determine and set up different secondary resonance patterns.

This will be studied by showing the insertion loss and reflection profile as a function of trace angle, routing scenarios and trace length for different glass-weaves.

2   Glass Weave Periodic Loading

The impact of a regular periodic change of the dielectric constant and loss on a trace can be understood using a simplified structure. The structure consisted of a stripline passing through a dielectric filled with resin and glass fabric (see Figure 1 (left)). Glass bundles were approximated by rectangular cross-sections, embedded in the resin and offset slightly from trace (see Figure 1 (right)). This unit-cell weave pattern can be stepped and repeated to form any trace length.

In reality, the weave geometry can vary significantly across style and suppliers, making it important to carefully select the range of simulation parameters. For example, Figure 2 (left) shows the approximate thickness of the uncompressed glass as if it were measured between to horizontal plates for a variety of glass styles; there is a large range of thickness values observed. On the right of Figure 2 the glass pitch for several glass styles is summarized [6]. These ranges provided the limits of the parametric simulation. One further complication is that some specifications are missing and need to be estimated; an example of this is the glass bundle width. These nominal values were estimated based on photographs of different glass styles and then swept around that value.
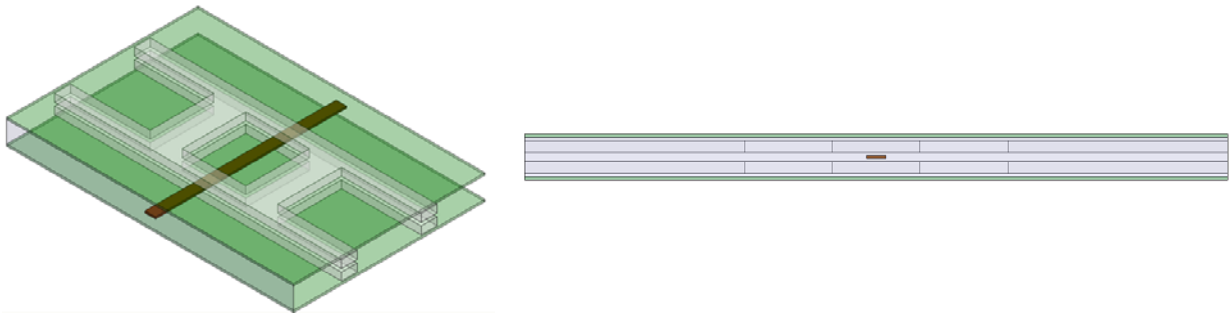

Figure 1 *Left:* Idealized stripline structure showing the glass weave pattern. For the glass, Dk and Df were 6 and 0%, respectively. For the resin, Dk and Df were 3.5 and 3%, respectively. The total trace length was 5 inches. *Right:* Cross-sectional view of the structure. The dielectric thickness above and below the trace remained constant at 4 mils. Each glass layer (nominally 3 mils thick) was centered symmetrically in the resin, on both sides of the trace, offset by 0.5 mils.

Glass Thickness of Various Styles

Glass Pitch of Various Styles
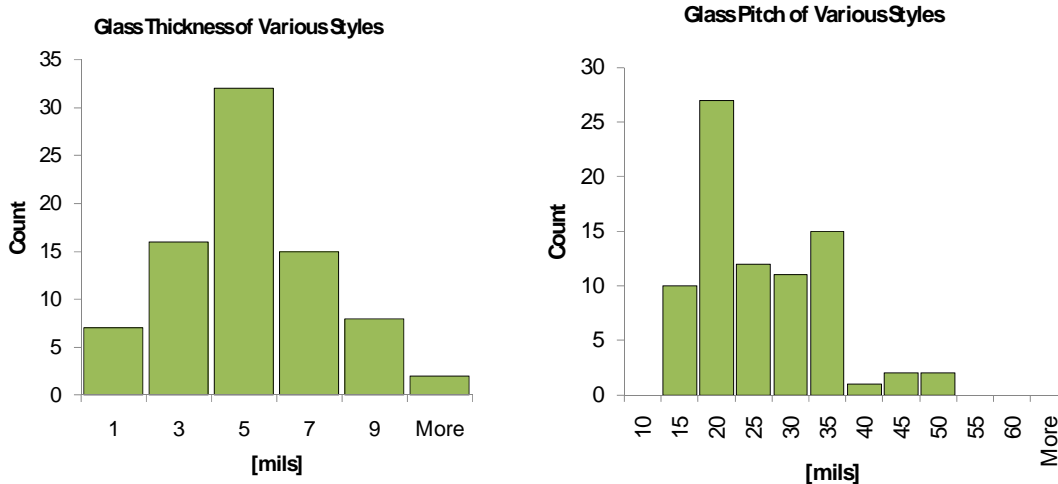
Figure 2 *Left:* Approximate thickness of the uncompressed glass. *Right:* Glass pitch for several glass styles.

Figure 3 shows a trace routing through a pin field and includes several types of trace sections which will be decomposed and analyzed separately: 0 degrees (a)-(c), 90 degrees (d) and 45 degrees (e). The figure shows that when the trace is routed at 0 or 90 degrees, three trace offset cases arise: (c) the trace is centered between horizontal glass bundles, (b) the trace is on top of a glass bundle or (a) the trace abuts the glass bundle. In this section, we concern ourselves with Cases (a)-(d) only. Case (e), as well as other route angles, will be investigated in a subsequent section.
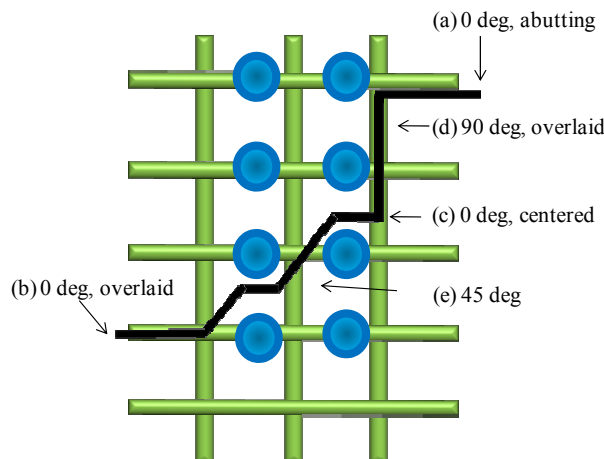
Figure 3 A trace jogging through a via pin field. Several types of line segments are identified.

Answers to a number of general questions were pursued in this first round of simulations such as: Can we see the impact of periodic loading of the glass weave? If so, at what frequencies does it introduce resonances? How does the width and thickness of the glass bundle influence these results? What if the glass bundles were offset from the trace surface? What is the influence of the positioning of the trace relative to the parallel glass

bundles? In the following paragraphs we summarize these simulation findings. Ansoft HFSS v12 was used for all field-solver simulations.

Figure 4 (left) plots the insertion loss for glass weave pitches of 20 and 60 mil. The width was maintained at 50% of the glass-weave pitch. By doing this, the effective Dk of the dielectric is approximately held constant. The first thing to observe in Figure 4 is that there is indeed a resonance due to the glass-weave periodic loading. Specifically, this resonance is a result of the periodic change of the dielectric constant and occurs where the distance between glass bundles is equal to one half a wavelength. We call the resonance due a single repeating unit cell (like shown in Figure 1) a *Single-Cell Periodicity* (SCP). Later on we will see that other periodicities are created when the trace doesn't cross the weave at only 0 or 90 degrees (or 45 degrees).

The 20 mil glass weave pitch resonance is too far out in frequency to be captured in the frequency range of the simulation. In Figure 4 (right) the 20 mil baseline is subtracted from the 60 mil insertion loss plot and this difference is plotted as a percentage of the 20 mil baseline insertion loss. This allows us to assess the roll off below the fundamental resonance in the insertion loss due to glass-weave periodic loading. The point here is that there is a gradual roll off from the baseline that can affect frequencies well below the fundamental. Subsequently we will see how these resonances can be pulled down to lower frequencies.

Figure 5 (left) shows the impact of the bundle width on the insertion loss. As the bundle width grows from 15 mils to 30 mils the magnitude of the resonance increases as the discontinuity grows. However, this trend does not continue indefinitely. At some point the opening in the glass weave is electrically small and the trace experiences a solid dielectric layer. Thus, in this extreme case, the glass-weave periodic resonance is eliminated as the transmission line would no longer be periodically loaded. Note that Figure 5 is illustrative and not realistic as the baseline loss is decreasing with increasing bundle width due to a decrease in the average Df. We can also see the shift in the resonant frequency due to the change in the effective Dk with width.
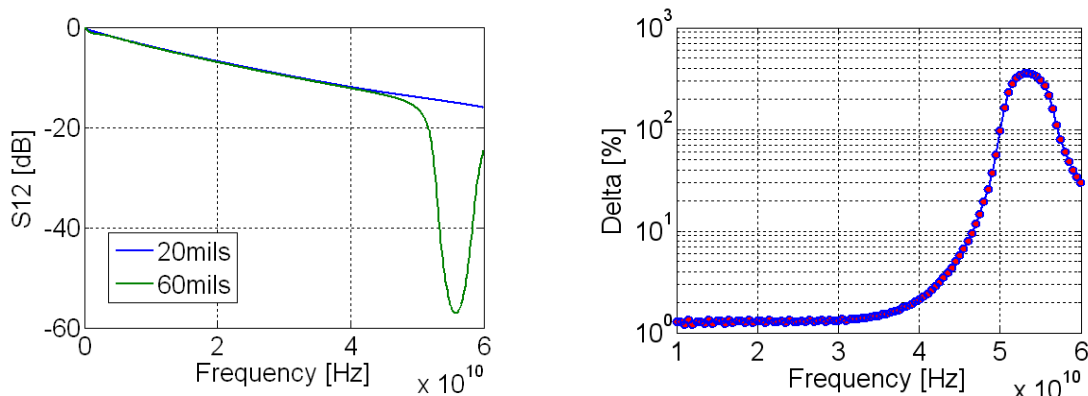

Figure 4 *Left:* Impact of bundle pitch on insertion loss. The bundle width was fixed at 50 % of the glass-weave pitch. *Right:* Additional loss of the 60 mil glass-weave pitch compared to the 20 mil glass-weave baseline. The trace length was 5 inches.
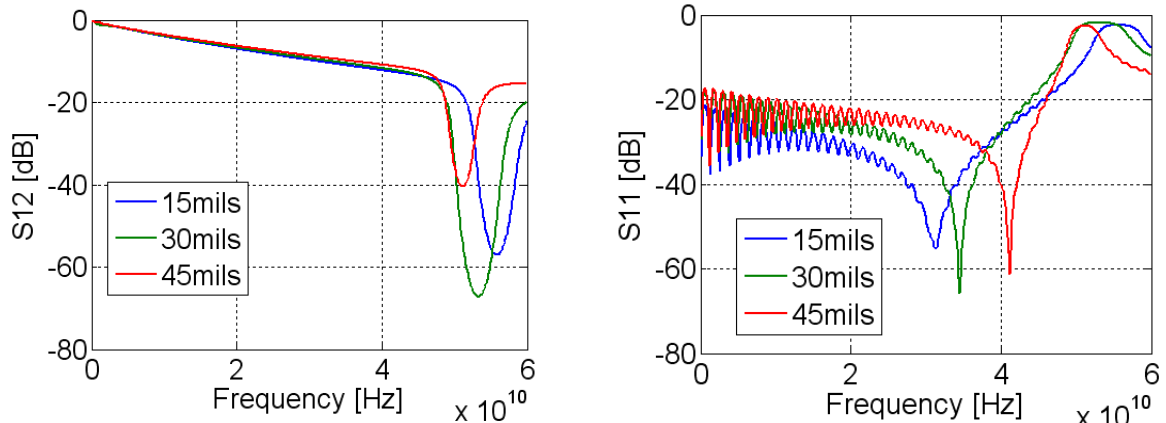
Figure 5 *Left:* Impact of bundle width on insertion loss. The bundle pitch was fixed at 60 mils. *Right*: Reflection profile for the three widths. The trace length was 5 inches.

Figure 5 (right) shows that the observed dips in the insertion loss profile correspond to peaks in the reflection profile, i.e. the dips are due to reflective loss.

Figure 6 shows the cross-sectional view of the structure used to examine the impact of glass thickness and the vertical offset of the glass from the trace. The glass-bundles ranged from 1-3 mils and were offset from the trace by 0-2 mils. Figure 7 shows the simulation results as glass-weave thickness and offset were swept. Several trends can be observed: the closer the glass-bundle is located to the surface of the trace, the greater the magnitude of the SCP resonance dip. We can also see from Figure 7 (right) that thicker glass-weaves (relative to the total thickness of the dielectric), will show a greater SCP resonance dip. Notice that a glass-weave that is only 25% of the total thickness still shows a dip.
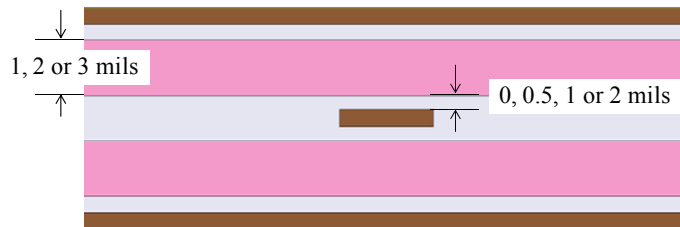

Figure 6 Cross-sectional view of the parameterized structure. Visible are the top and bottom planes, signal conductor, and the upper and lower glass bundles with surrounding resin.
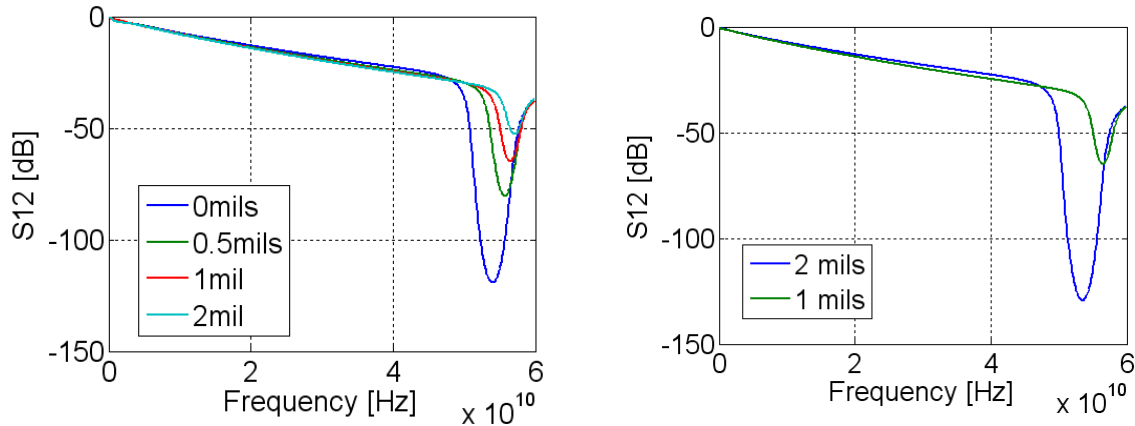
Figure 7 *Left:* Impact of glass weave vertical offset from the trace on insertion loss. *Right:* Impact of weave thickness on insertion loss. The weave remained vertically centered between the trace and the plane as the thickness was swept. The trace length was 5 inches.

Finally, we examine how the positioning of the trace relative to the parallel glass bundles impacts the SCP. Three cases were considered: Case (c), where the trace is centered between horizontal glass bundles, Case (b), where the trace is on top of a glass bundle and Case (a), where the trace abuts the glass bundle. The simulation results shown in Figure 8 are somewhat expected; with the trace centered between the glass bundles, Case (c), the SCP resonance dip has the greatest magnitude. By arranging the trace parallel and just touching a horizontal glass bundle, i.e., Case (a), the resonance dip is reduced. This happens because a portion of the trace field distribution now comes in contact with a uniform dielectric and the periodic loading is so to speak averaged with this uniform region. Lastly, the SCP is eliminated entirely in Case (c) as the trace is no longer periodically loaded and experiences a uniform dielectric glass dielectric[1].
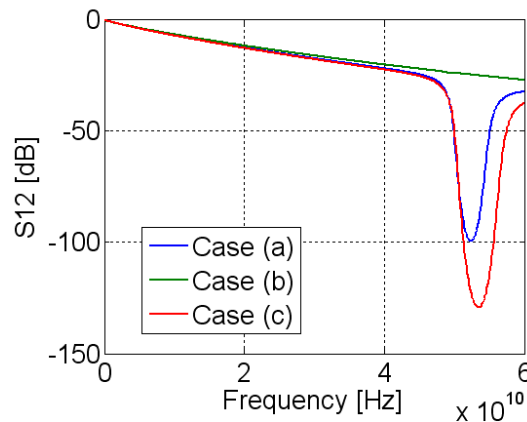
Figure 8 Impact of parallel bundles on glass weave periodic loading.

---

[1] Strictly speaking there is still periodic loading due to the crossing bundles further away from the trace, but it becomes negligibly small.

Several of the simulations above were repeated using the much more realistic glass-weave representation used in [2]. Although these simulations took much longer to run due to the detailed weave geometry, they were undertaken to ensure that we weren't oversimplifying the glass-weave geometry and that the resonances and dependencies observed above were still valid.

Below we summarize several key findings from this section:

- The glass weave resonance frequency corresponds to the half wave resonance distance between bundles (pitch).
- Although the resonance frequency can be relatively high (dependent on the bundle pitch) there is additional low frequency loss due to this resonance.
- Wider bundles tend to increase the size of the periodic resonance until the window in the glass-weave is electrically small whereupon trace is not periodically loaded.
- Increased weave thickness and vertical proximity to the trace increases the periodic loading due to the glass-weave.

3   Impact of Trace Route to Glass Weave Angle

In the previous section we looked at the impact of a stripline trace crossing at 0 or 90 degrees to the glass weave, i.e., Cases (a)-(d). Glass weaves are typically oriented parallel to the *board edge* (nominally). As a consequence, any trace route that is not parallel to the board edge will likely intersect the glass weave at some angle, e.g., Case (e) or 45 degrees. Even if a trace is also routed parallel to the board edge and is approximately parallel to the glass bundles, there will likely be some small angle between the glass bundles and the trace. In this section, we will examine the impact of trace routes at an angle other than 0 and 90 degrees. Specifically, because of the symmetry of a *square* glass weave pattern we will concern ourselves with a trace route angle ranging from $0 < \theta \leq 45$. The impact of rectangular glass weave patterns will be considered separately. Furthermore, we concern ourselves with *straight* trace routes in this section, or trace routes that are routed at a fixed angle relative to the glass weave from its source to its destination. The proceeding section will examine the impact of *meandering* trace routes.

A simulation environment was created in Matlab to study the impact of the weave with different route angles. The algorithm followed was:

1. Place a trace on a square grid and look at all intersection points on vertical and horizontal bundles for a given route angle, glass-weave pitch, and trace length
2. Calculate the distance between neighboring intersections
3. Sweep route angle and trace length (and glass-bundle pitch)
4. Post-process results

The benefit of this approach is that it leverages our understanding from the prior section and abstracts it, allowing for an efficient analysis of a large number of cases. The

inherent assumption in this analysis is that the glass bundle thickness and trace thickness are infinitely thin. This means, for example, that traces passing over glass bundles which are very wide (relative to the glass-weave pitch) would not necessarily see this exact behavior.

Figure 9 shows an example of the output of the script (from Step 1, above) consisting of a glass-weave grid with overlaid traces in 10 degree steps. A couple of features can be observed from the figure: first, 0, 45 and 90 degree routes will result in no more than a single periodicity on a straight trace. For other route angles, more than one periodicity can arise. Also notice that the periodicity of a 45 degree route will always be longer than a 0 or 90 degree route on a square grid. Lastly, notice the effect of trace length: the trace closest to 90 degrees has not yet intersected a vertical bundle over 500 mils. It may take several inches for the periodic nature of the weave to show up. Put another way, it will take a relatively longer trace to arrive at the final distribution of bundle crossings as you get closer to 90 degrees.
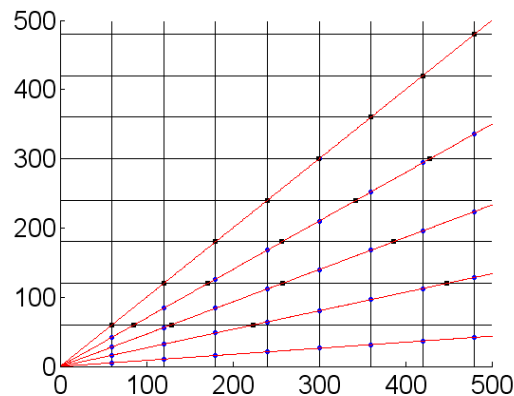

Figure 9 Example glass-weave grid (black) with overlaid traces (red) at 10 degree steps. Black dots are horizontal bundle crossings. Blue dots are vertical bundle crossings. The grid pitch is 60 mils. The units are in mils.

Figure 10, Row (a) shows (moving from left to right) the histograms of the distance between neighboring intersections for a trace route angle of 50, 70, and 85 degrees. The trace length is 5 inches. Notice that as the trace is routed closer to 45, the distribution becomes flatter, with many different intersection distances. Conversely, as the trace is routed closer to 90 degrees, a single intersection distance dominates the distribution.

Figure 10, Row (b) shows the equivalent SCP frequency for each of the three route angles. Notice that the minimum SCP frequency decreases as the trace gets closer to 45 degrees. In fact, 45 degrees is the route angle which creates the lowest SCP resonant frequency. Thus although Figure 2 (right) shows a distribution of glass weave pitches which would normally dictate the SCP resonance frequency, by routing on a 45 degree angle across the glass weave we effectively grow the pitch by $\sqrt{2}$. It's interesting to point out that routing on a 45 degree angle is often the recommended approach to avoid differential pair skew and asymmetry.

The final row of Figure 10 shows the intersection distances as you move along the trace path. What is very interesting here is that as the route angle approaches 90 degrees, the *horizontal* bundle crossings are widely separated. In fact, these crossings get further and further separated as you approach 90 degrees. If we think of this in terms of unit cells (i.e., building blocks which can be stepped and repeated), the unit cell would now need to be much longer to properly capture the horizontal bundle crossings. Because the unit cell is longer, a much lower frequency periodic loading is created, one that spans multiple cells. We call this type of periodic loading: *Multi-Cell Periodicity* (MCP). This distinguishes it from a SCP which can occur at a higher resonance frequency, dictated only by the weave pitch.
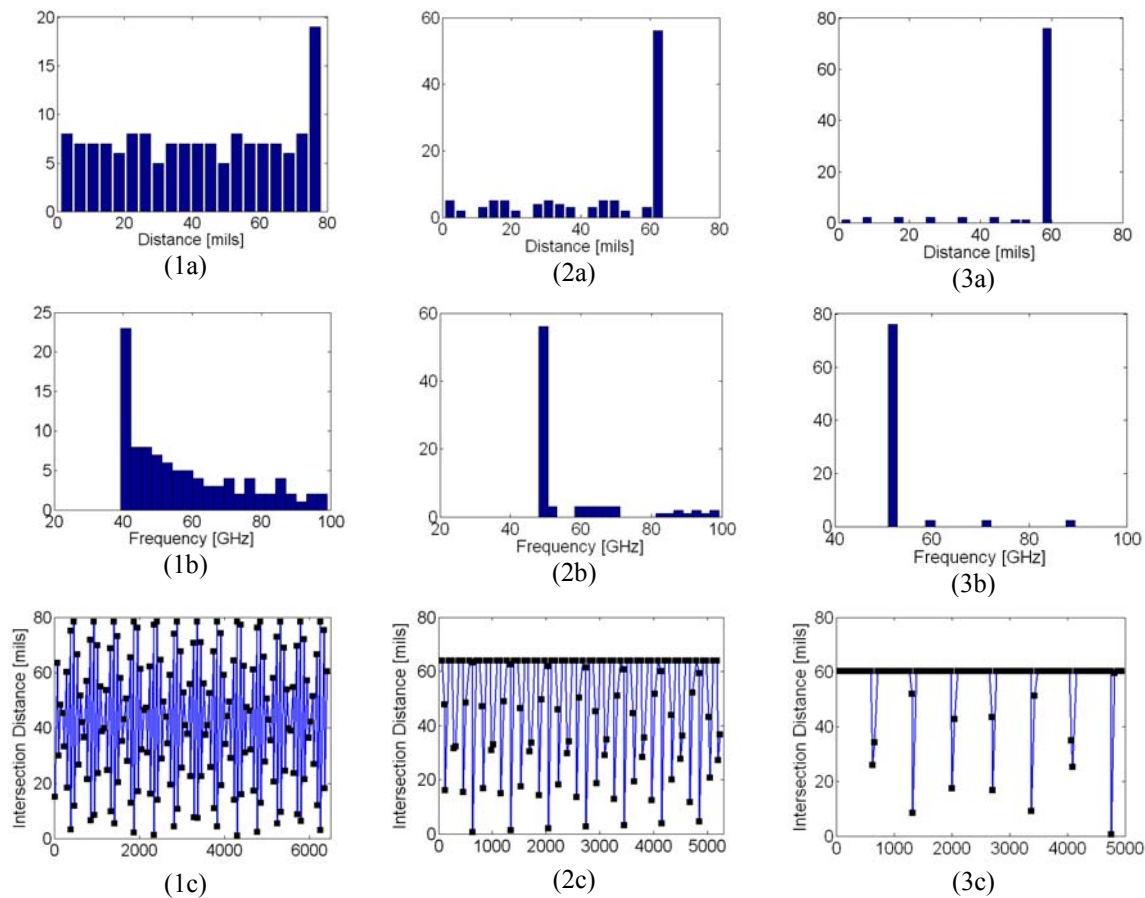
Figure 10 *Row (a):* Histograms of the distance between neighboring intersections for a trace route angle of 50 (1a) , 70 (2a), and 85 (3a) degrees. *Row (b):* Histograms of the equivalent SCP frequency for a route angle of 50 (1b), 70 (2b), and 85 (3b) degrees. *Row (c):* Intersection distances as you move along the trace path for the 50 (1c), 70 (2c) and 85 (3c) degree routes. The x-axis shows the number of intersections, not the length of the trace.

Figure 11 plots the points of intersection on the *horizontal* bundles for different trace route angles (black dots). Again we see that aside from the 45 degree route, these

crossings occur much less frequently than the vertical glass bundle crossings. An interesting visual pattern arises from the family of different trace crossings as they get closer to 90 degrees. We see that these horizontal crossing are periodic, just over a much longer distance compared to the vertical bundle crossings.
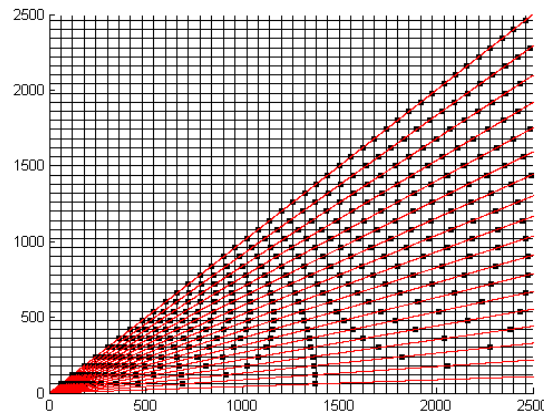

Figure 11 Example of glass-weave grid (black) with overlaid traces (red) at 2.5 degree steps. *Only horizontal glass bundle crossings are shown*. The grid pitch is 60 mils. The units are in mils.

Figure 12 plots the MCP resonance frequency for a 2.5-inch long trace as a function of route angle and glass-weave pitch. Overall, we see that glass-weave pitch and route angle determine the MCP resonance frequency (as well as the dielectric constant). For a given glass-weave pitch, the resonance frequency is almost linear with the route angle. The lowest MCP resonance frequency occurs with widely pitched glass-weaves and trace route angles close to 90 degrees (right corner of the graph).
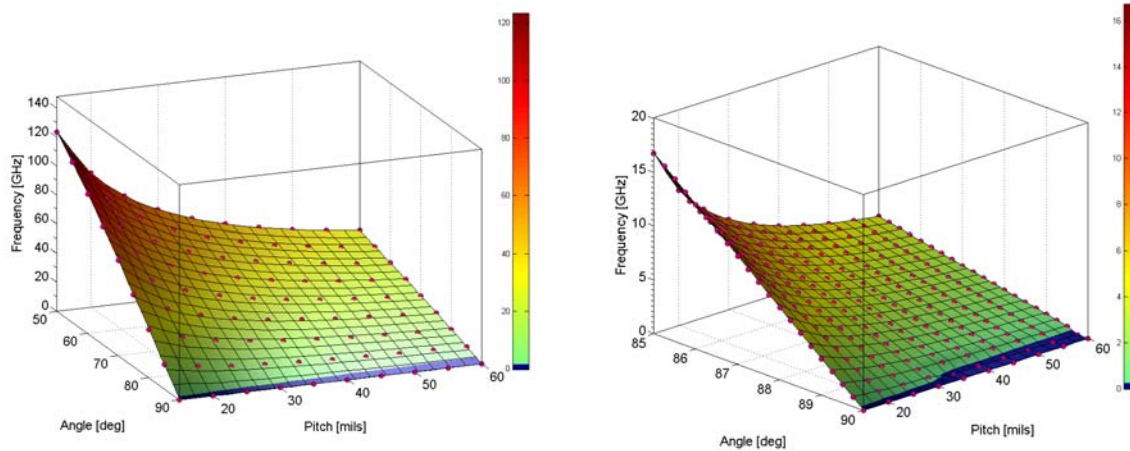
Figure 12 (right) is a more detailed simulation run of the left, focusing on the 85-90 degree route angles. Notice the dark blue flat region on Figure 12 (right), which is also shown as a sliver of blue on the bottom of Figure 12 (left). This is where the combination of route angle, glass-weave pitch and trace length prevent a MCP from being established. This will always happen for 90 degree routes and we can see that for a given route angle and length, wider glass pitches will prevent MCP from being established.

Figure 13 shows the same types of plots for Figure 12 except for a 7.5-inch long trace. Comparing Figure 12 (right) and Figure 13 (right), we notice how much larger the dark blue flat region is in Figure 12. What this means is that for a given trace route angle and glass-weave pitch, a shorter trace route will prevent MCP from being established. This makes intuitive sense as the shorter route will have less overall bundle crossings for a given trace route angle and glass-weave pitch.
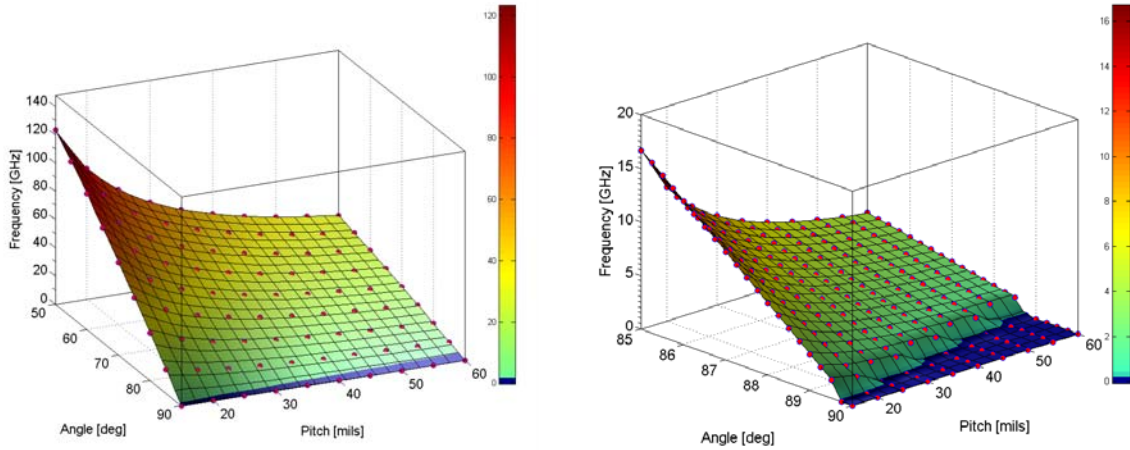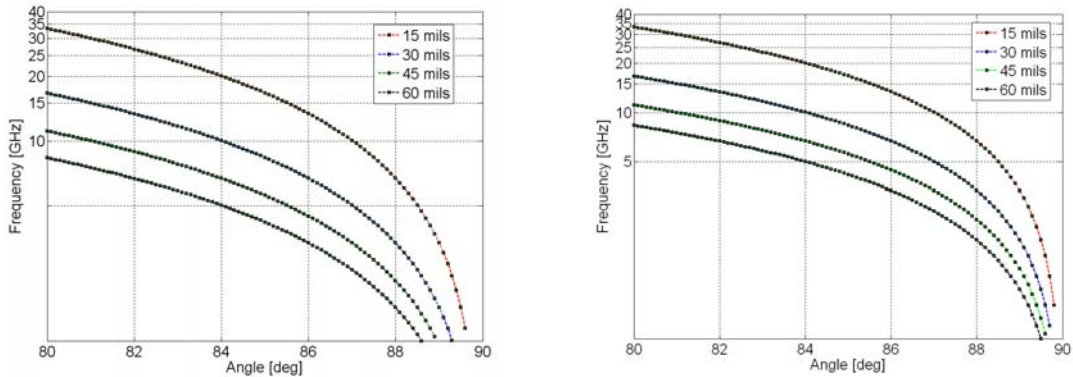
Figure 12 Surface plot of the MCP resonance frequency for a 2500 mil trace routed at 50-90 degrees (*left*) and a more detailed simulation run focusing on 85-90 degrees (*right*) using glass-weave pitches ranging from 15-60 mils. The red dots are simulated values whereas the surface is interpolated.

The dependency of the resonance frequency on glass-weave pitch and trace route angle is shown on a two-dimensional plot in Figure 14. The trace length was 2.5 inches (left) and 7.5 inches (right). Comparing the two figures, we see the point at which each curve drops off (i.e. the MCP cannot be established) is pushed further to right with increasing length. This means, for example, that even a trace with a routing angle very close to 90 degrees, would eventually set up a MCP if the trace is sufficiently long.

Figure 13 Surface plot of the MCP resonance frequency for a 7500 mil trace routed at 50-90 degrees (*left*) and a more detailed simulation run focusing on 85-90 degrees (*right*) using glass-weave pitches ranging from 15-60 mils. The red dots are simulated values whereas the surface is interpolated.

Figure 14 Plot of the MCP resonance frequency for a 2.5-inch trace (*left*) and 7.5-inch trace (*right*) routed at 80-90 degrees using glass-weave pitches ranging from 15-60 mils.

Lastly, if we modify the grid to now be rectangular we find that many of the trends observed above remain the same but some new possibilities arise. For example, we will get a bimodal distribution in Figure 10, row (a), if the weave is 60 mils by 40 mils, for example, thus creating a MCP that is almost three times as long as trace routed on the 45 of a square grid. It's even possible to avoid having multiple intersection distances on the forty-five with a non-square grid; for example, a 60 mil by 30 mil grid will set up only one periodicity.

Below we summarize several key findings from this section:

- The lowest possible SCP is with a 45 degree route for a square grid
- When the angle between the glass and trace is other than 0, 45 and 90 degrees it is possible to observe a much lower frequency periodic loading. This type of periodic loading is called *Multi-Cell Periodicity* (MCP).
- Glass-weave pitch and route angle determine the MCP resonance frequency (as well as the dielectric constant).
- The lowest MCP resonance frequency occurs with widely pitched glass-weaves and trace route angles close to 90 degrees.
- MCPs can still occur on non-square grids.

4   The Impact of Meandering Trace Routes

In the previous section we introduced the concept of a MCP where resonances are created when the trace is slanted with respect to the glass bundles, creating periodicity over several or many glass-weave cells. In fact, a MCP can be introduced even if the trace is not slanted due to the trace routing itself. Consider a trace routing through a BGA pin field with plated through hole (PTH) vias (see Figure 15, which shows a top view). As

the trace passes through the pin field, it is forced to jog around the vias, as shown in Figure 15. This creates another type of MCP: the jogs in the trace route disrupt the simple repeating pattern creating a multi-cell periodicity. This can introduce resonances at much lower frequencies than SCPs; for example, if the SCP was 50 GHz in Figure 15, it would be pushed down to 12.5 GHz by the MCP on the right. Of course, if the trace route is not easily broken down into unit cells, as described here, and instead the trace route is irregular, the resonances would not have the chance to build at one particular frequency and this phenomenon might be smaller in magnitude but widened in frequency.
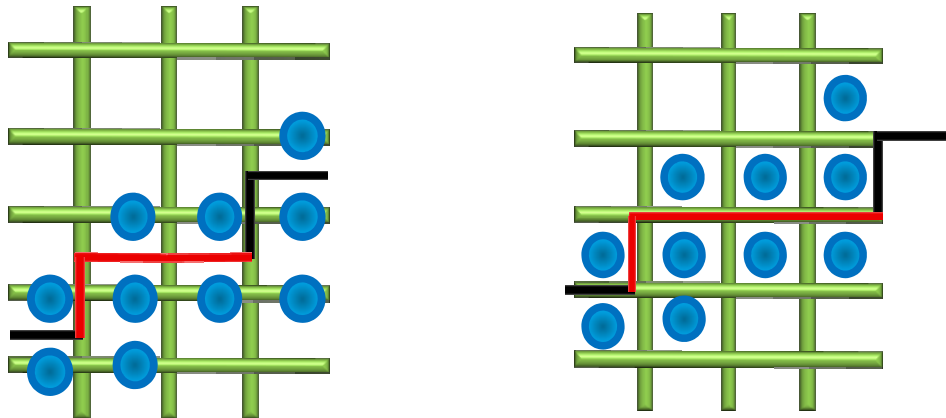

Figure 15 Two different possible scenarios for a trace routing through a 1 mm BGA pin field. The glass-weave pitch is 40 mils. The trace is forced to jog around the PTH vias creating a MCPs that spans 3*40 mils (*left*) and 4*40 mils (*right*). The unit cell is highlighted in red.

5   Test Structure Measurement

A test board was designed which consisted of a number of 14-inch long differential pairs routed parallel to the board edge on different routing layers and at different pitches. Figure 16 shows a portion of the board layout (right) and a photograph of the top end of the traces showing the wafer probe used for the measurements (left).

In order to measure the stripline traces, the test board was milled down all the way to the stripline area exposing the copper surfaces. Differential 500 um GSSG wafer probes were used at each end of the differential lines, and measurements were taken using an Agilent 4-port VNA with a linear sweep ranging from 300 KHz to 20 GHz with 1601 points. The measurement setup was calibrated at the end of the wafer probe tips using a SOLT wafer calibration substrate. A large number of the differential pairs at different pitches were measured.
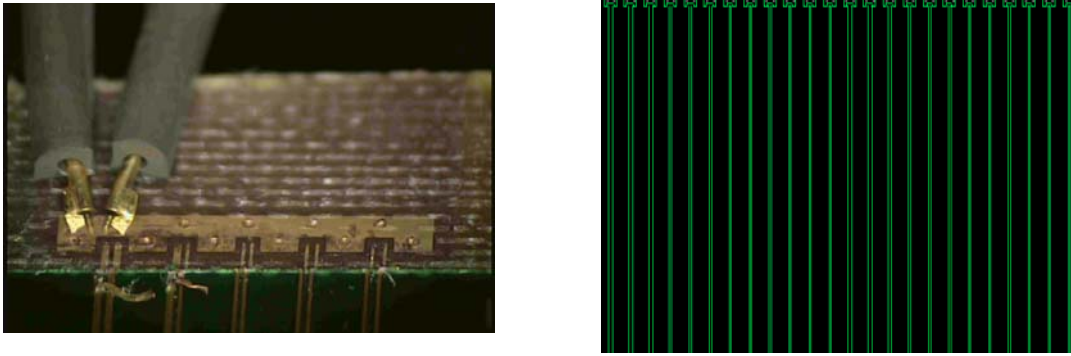
Figure 16 *Left:* Photograph of the top end of the traces showing the wafer probe used for the measurements. *Right:* Snapshot of the board layout showing the wide array of trace pitches and widths that were measured.

Figure 17 shows the measured single-ended insertion loss data on two boards: board #1 (left) and board #2 (right). Figure 18 and Figure 19 show the mixed-mode insertion loss and single-ended return loss, respectively, for the two boards. Looking at both the single-ended and mixed-mode insertion loss profile we see that board #1 and #2 show resonance dips at 11.1 GHz and 8.9 GHz, respectively. At first it was suspected this might be due to a calibration issue so these measurements were repeated many months later with a totally different VNA unit and using a new calibration. The resonant dip was still present and the measurements showed good agreement with the previous measured data. The return loss plots (Figure 19) show a corresponding peak at the same frequency, indicating the dip is due to reflective loss. This agrees with our earlier simulation results (Figure 5 right) and is consistent with a glass-weave reflection.
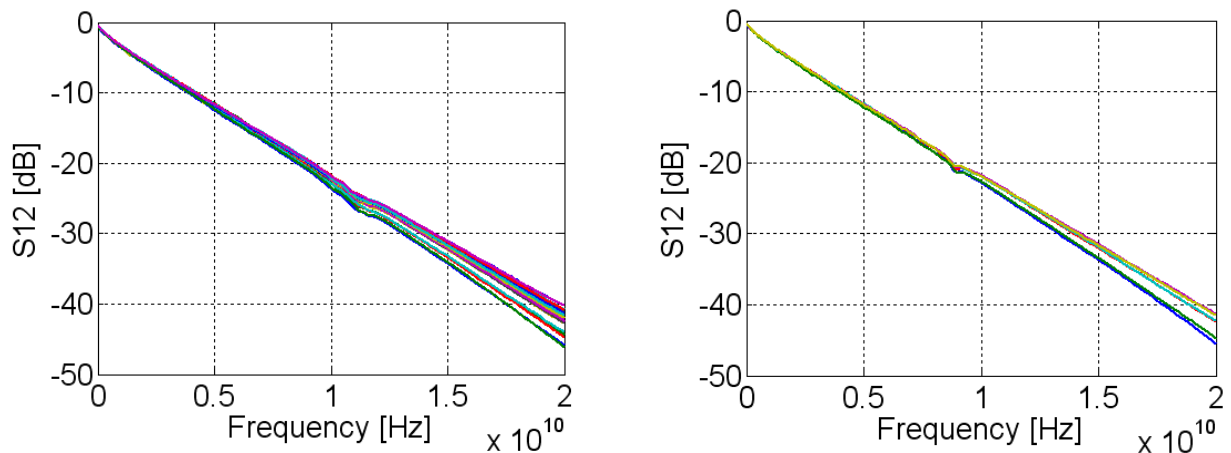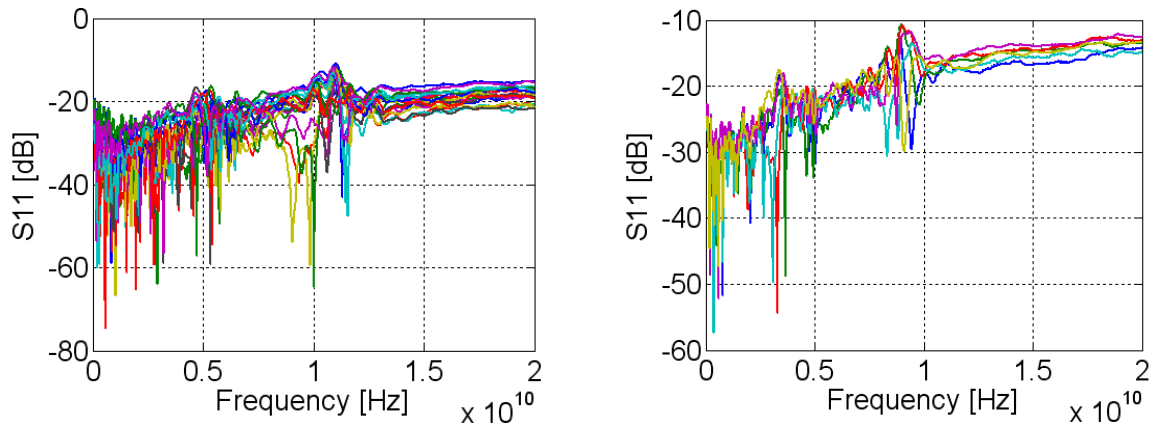

Figure 17 Measured single-ended insertion loss for board #1 (left) and board #2 (right).
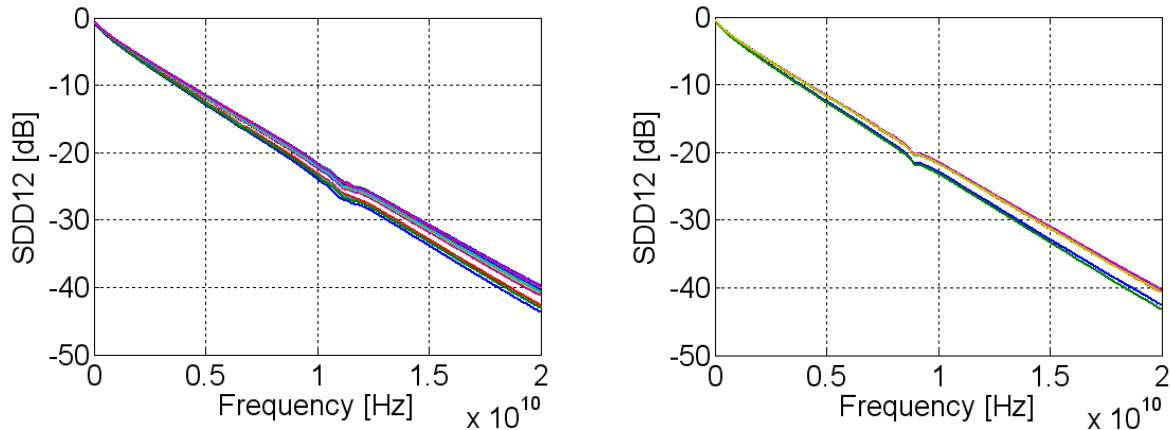
Figure 18 Measured mixed-mode insertion loss for board #1 (left) and board #2 (right).


Figure 19 Measured single-ended return loss for board #1 (left) and board #2 (right).

After VNA measurements of the s-parameters, the test boards were milled down (Figure 20) from opposite sides to a location such that the glass-weave was exposed and the trace below was still visible (Figure 21). This allowed us to visually determine the trace to glass-weave routing angle along the entire length of the trace. The relationship between the trace and the weave can be independent on the dielectric layer above and below the trace, which is one reason why the board needed to be milled from both sides. Furthermore, the glass-weave styles were different above and below the stripline: on the top it consisted of 1080 x 2 and below it was 2116 x1.

Milling from the opposite side proved to be a more tedious process than milling only from the top of the board where the board needed to be milled down to only ~10 mils. Supports were required to prevent the milling bit pressure from deforming the board and constant adjustments were made to control the precise milling depth. This resulted in a fairly planar milling depth (approximately +/- 2 mil) across 14 inches.

Figure 20 Photograph of the milling machine and secured board. Careful adjustments and measures were taken which allowed the board to be milled in approximately one-mil increments.
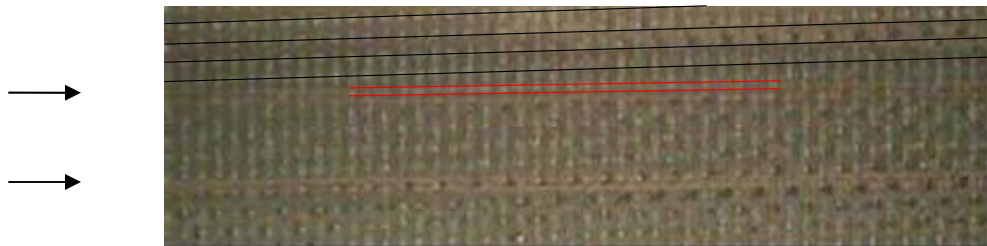

Figure 21 Photograph of glass-weave with two differential pairs (arrows are aligned with the two differential pairs and a portion of the upper pair is highlighted in red). The angle of the weave relative to the trace is apparent and several horizontal glass bundles are highlighted in black.

The change in glass-weave routing angle as a function of a differential pair trace length is shown in Figure 22. The trace to glass-weave orientation is nominally oriented like Case (c) from Figure 3 (i.e. 90 degrees) but a slight angle in the glass-weave causes the glass-bundles to eventually intersect the differential pair. Originally we believed that the trace to glass-weave routing angle would be relatively constant for the length of the trace. In fact, what we see is that there are some sections where the angle is very slight (only ~0.5 degrees less than 90) and other regions have considerable deviation from 90 degrees (~86.5 degrees). These findings are consistent with [7] which found very little evidence for differential propagation differences despite a fairly exhaustive search, i.e. differential propagation differences would only be manifest if either of the traces ran parallel to the glass bundles for some significant portion of the length.

Figure 23 creates a histogram of the measured deviations from 90 degrees.
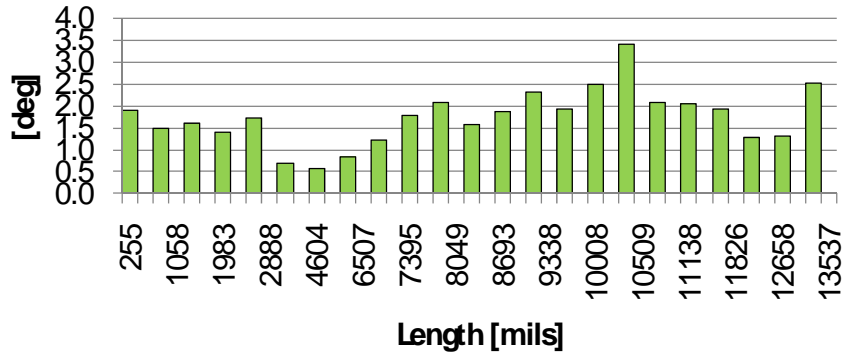
Figure 22 Measured change in trace to glass-weave routing angle as a function of a differential pair trace length. The y-axis is the deviation from 90 degrees.
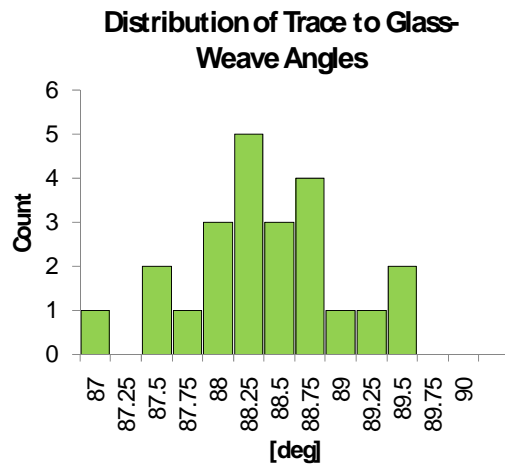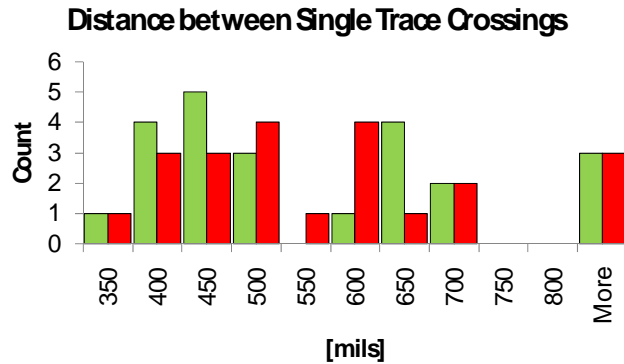

Figure 23 Distribution of measured trace to glass-weave routing angle of a single differential pair.

Another physical measurement that was taken is the number of intersection points on both sides of a differential pair along the length of the trace (Figure 24). Only horizontal glass bundle crossings are captured. Figure 25 shows a distribution of the intersection distances between crossings on a single trace. The distribution shows each leg of the differential pair separately. Notice how broad the distribution is.
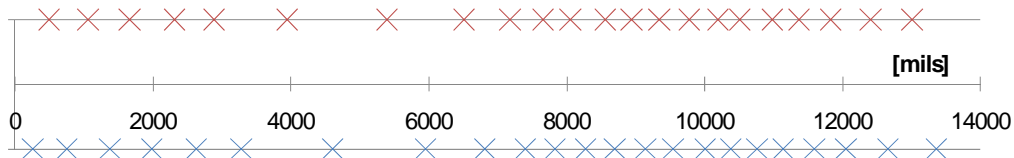
Figure 24 Measured location of the intersections with a horizontal bundle on each side of the differential pair along the length of the trace. Red 'x' and blue 'x' indicate where the weave crossed over the trace. Only horizontal glass bundle crossings are captured.

Distance between Single Trace Crossings

Figure 25 Distribution of measured intersection points on each side of the differential pair along the length of the trace. Green and red bars represent separate sides of the differential pair.

Figure 22-Figure 25 are data from the glass-weave on the top of the trace on board #2. Figure 26 (right) shows the distribution of intersection points for the top *and bottom* glass-weave with one side of the differential pair for the same board. Red and green bars represent the intersections with the top and bottom glass-weaves, respectively. Figure 26 (left) shows the same type of plot but for board #1. Comparing the two qualitatively, notice that the crossing are overall longer in board #2.

Figure 27 plots the equivalent resonant frequency for the intersection distances shown in Figure 26 for the top and bottom glass-weaves. The resonance frequencies were calculated using the extracted dielectric constant from the group delay of the measurement data and assuming a half-wave resonance is established between the glass bundles. I.e., these resonances are due to MCPs arising from the horizontal bundle crossings. We see that in order to get the full picture of trace crossings and resonances we must combine the upper and lower glass-weaves. If we pick a visual center for the distribution on the right, it would be about 9 GHz, which lines up nicely with the dip observed in Figure 17 (right) and Figure 18 (right).

Although the top glass-weave distribution has a similar frequency profile for the two boards (in red), notice that the bottom glass-weaves are different (in green); specifically, board #1 (left), has higher frequency components compared to board #2. This also correlates to the measured data seen in Figure 17 (left) and Figure 18 (left) where the insertion loss dip is observed to be about 2 GHz higher in frequency for board #1.

Further simulations would be required to *quantitatively* correlate the measured dip to the distribution of glass-weave crossings. These simulations would need to account for the physical location of the glass-weave crossings along the length. Reflections can cancel or build depending on how these crossings are distributed along the trace. Moreover, these simulations would need to combine the effect of the crossings on the two separate dielectric layers. Time limitations did not permit us to undertake these simulations.
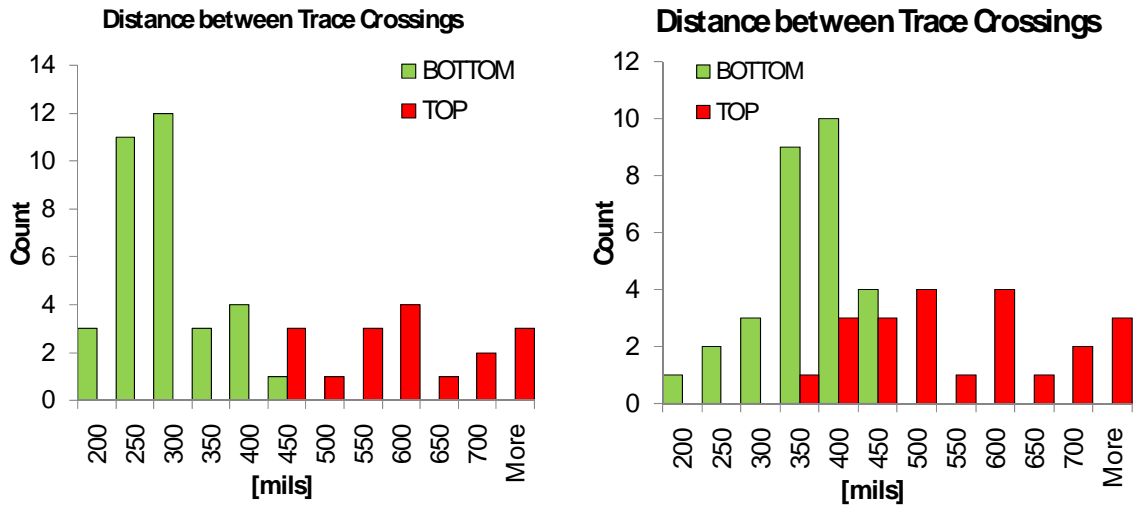
Figure 26 Distribution of intersection points between the top and bottom glass-weave with one side of the differential pair for board #1 (*left*) and board #2 (*right*).. Green and red bars represent the intersections with the top and bottom glass-weaves, respectively.
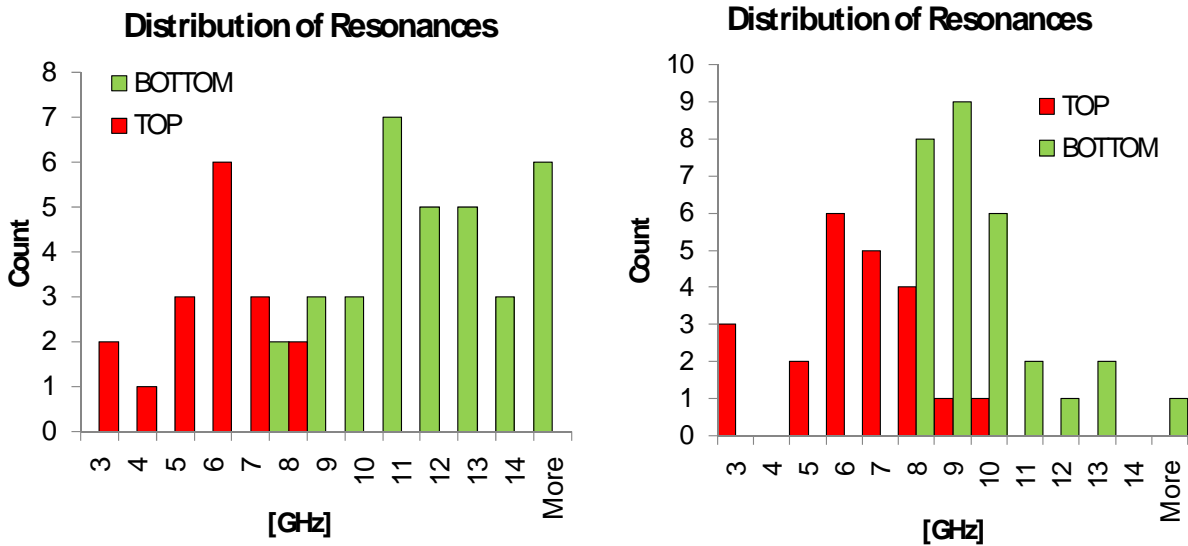
Figure 27 Distribution of resonant frequencies calculated from the measured intersection distances in Figure 26 for board #1 (*left*) and board #2 (*right*). Green and red bars represent the resonances from the top and bottom glass-weaves, respectively.

Below we summarize several key findings from this section:

- Trace to glass-weave routing angle can vary by layer and can be different above and below the trace.
- Trace to glass-weave routing angle can vary along the trace length
- A wide distribution of resonances can be introduced due to the variation in glass-weave angle along the trace's length.

- Measurement results showed an insertion loss dip at two different frequencies on two otherwise identical boards, which showed reasonable to the distribution of glass-weave trace crossings.

6   Conclusions

In this study we have identified a new trace loss mechanism due to the glass-weave periodicity. Two new terms were defined and introduced to help speak about these types of periodicities: a single-cell periodicity (SCP) and multi-cell periodicity (MCP). SCP originates from the pitch of the glass weave itself. Although the resonance frequency due to SCP can be high when considering today's bandwidth requirements, we showed there is an additional steepening of the loss profile slope, well below this fundamental resonance, due to the resonance dip. MCPs are introduced when longer range unit cells are established due to the trace to glass-weave angle. These resonances can occur at a much lower frequency than SCPs. It was also discussed that simple trace jogs can introduce their own MCP even if the trace is routed parallel to the glass-weave (no trace to glass-weave angle).

Detailed physical measurements were taken on different boards and we found that trace to glass-weave routing angle can vary by layer and along the entire length of the trace. Furthermore, the glass-weave angle can be very different above and below the trace. Measurement results showed an insertion loss dip at two different frequencies on two otherwise identical boards, which correlated well to the distribution of these glass-weave trace crossings measurements. Although the overall magnitude of the dip was small, the observed random nature of the weave does not preclude other more worrying distributions from arising, such as narrow distributions where the glass-weave crosses at regular, widely-spaced intervals.

In terms of practical implications, we found that although best practices dictate that 45 degree routes are preferred to reduce or eliminate differential skew due to glass weave effects, this strategy does not avoid the additional losses due to glass-weave periodic loading and in fact it results in the lowest SCP frequency. On the other hand, it was found that 0 and 90 degree routes have their own set of issues as small route angle differences between the glass weave and the trace can introduce MCPs.

Overall, one possible way to mitigate the effects of glass-weave periodicity is to require suppliers to reduce the glass-weave 'window' opening, i.e. by tightening the weave. The further the glass fabric is spread out, the more electrically uniform the dielectric will be. There may also be additional benefits to this approach including more consistent laser and mechanical drilling. Until those glass styles become available, it is not advisable to keep the same routing angle, it should be randomized. Unfortunately, if the total length is a concern, zigzagging the trace will only increase the length further, otherwise it would help in fighting this phenomenon. Periodicities due to large pin fields (under BGAs, connectors, etc.) – as briefly discussed in Section 4 – can be minimized by altering the jogging pattern through the pin field.

References

1. Scott McMorrow, Chris Heard, "The Impact of PCB Laminate Weave on the Electrical Performance of Differential Signaling at Multi-Gigabit Data Rates," DesignCon 2005, Santa Clara, CA.
2. Chris Herrick, Thomas Buck, Ruihua Ding, "Bounding the Glass Weave Effect through Simulation," DesignCon 2009, Santa Clara, CA.
3. Fred Gardiol: Lossy Transmission Lines. Artech House, Norwood, MA, 1987.
4. Gustavo Blando, Jason R. Miller, Istvan Novak, Jim Delap, Cheryl Preston, "Attenuation in PCB Traces due to Periodic Discontinuities," DesignCon 2006, Santa Clara, CA.
5. Jason R. Miller, Gustavo Blando, Istvan Novak, "Crosstalk due to Periodic Plane Cutouts," DesignCon 2007, Santa Clara, CA.
6. IPC-4412A, Amendment 1, Specification for Finished Fabric Woven from "E" Glass Printed Boards, March 2008.
7. Gustavo Blando, Jason R. Miller, Istvan Novak, " Losses Induced by Asymmetry in Differential Transmission Lines," DesignCon 2007, Santa Clara, CA.